

## Implementation of Intense Pulse Light output as pulsed shapes- pulse superposition for skin lesions

Jeun-Jong Baeg<sup>1</sup>, Han-Ho Tac<sup>2</sup>, Whi-Young Kim\*

<sup>1</sup>(Department of Electronic engineering, Gyeongnam National University of Science and Technology, Korea

<sup>2</sup>( Department of Electronic engineering, Gyeongnam National University of Science and Technology, Korea

<sup>\*</sup>(Department of Biomedical Engineering Dongju college University, Korea)

---

**ABSTRACT:** Strong demand exists for an Intense Pulse Light (IPL) that consists of a wide range of wavelengths from UV to IR by installing a nonlinear optic material on the IPL output unit. A nonlinear optic device, which uses the IPL with a high harmonic wave and parameter generating device by changing frequency, is being used extensively. Nonlinear optic response of the optic medium in each of the new frequency range can be applied. These procedures can be advantageous when utilizing the high power radiation in the range from UV to IR. The optic parameter generator and amplifier generate two types of wavelengths in the low frequency range. This can be utilized from a single frequency in the visible ray domain to the one in the UV region. In this study, a green light was obtained by attaching the SHG device, which was manufactured with the standard waveform using a multiple pulse overlapping circuit, and the conversion efficiency based on the correlation between the green light output and the one where energy was permitted in the overlapping circuit were examined.

**KEYWORDS:** Intense Pulsed Light, AVR, Xe Lamp, pulse shapes, pulse superposition

---

### I. INTRODUCTION

The IPL currently used in the medical field is 3.4cm in width and 0.8cm in length, which gently emits the rays onto the overall facial area. The application of an IPL is becoming extensive because a nonlinear optic material can be installed at the output unit so that it emits the IPL beam with a wide range of wavelengths. In particular, the IPL infiltrates deep into the skin, imparting elasticity to skin collagen and rejuvenating it. The IPL also causes epidermal peeling due to vascular changes in the dermis and its effects on fibroblasts. Measurements taken using the IPL beam contribute strongly to scientific development because it can measure more than the existing devices. In terms of the IPL treatments, the treatment effects of the IPL beam or its pulse forms can have a strong influence on the heat-physical interaction, depending on the skin condition, even if the same input energy is permitted. An IPL with a variable wavelength is normally used in cosmetic dermatology because it brightens the skin tone and softens the skin texture.

The variable wavelength-IPL in the past had a short life and is relatively heavy-duty, making it unsuitable for medical treatment, processing skin information, or for skin disease. Recently, a small-sized long lasting IPL beam with a wide range of wavelengths, from the visible ray to UV, was found by installing nonlinear optic crystals in the output unit of the IPL. KDP and LAP, which are both nonlinear optic crystals, can grow large enough to be used in large-sized IPL systems, BBO and LBP are used for the large output and high repetition type of IPL, and KTP is used for small output IPL.

The KTP crystal is a special type of nonlinear optic crystal that is used extensively in Second Harmonic Generation (SHG) of IPL, which generates a wavelength of approximately 1  $\mu\text{m}$ . Therefore, in this study, an attempt was made to obtain a variable efficiently or green light in the desired pulse form by installing a KTP in the IPL output unit so that the overlapping method can be applied in cases where the skin tone and texture are needed.

## II. MATERIALS AND METHODS

### 2-1. Composition

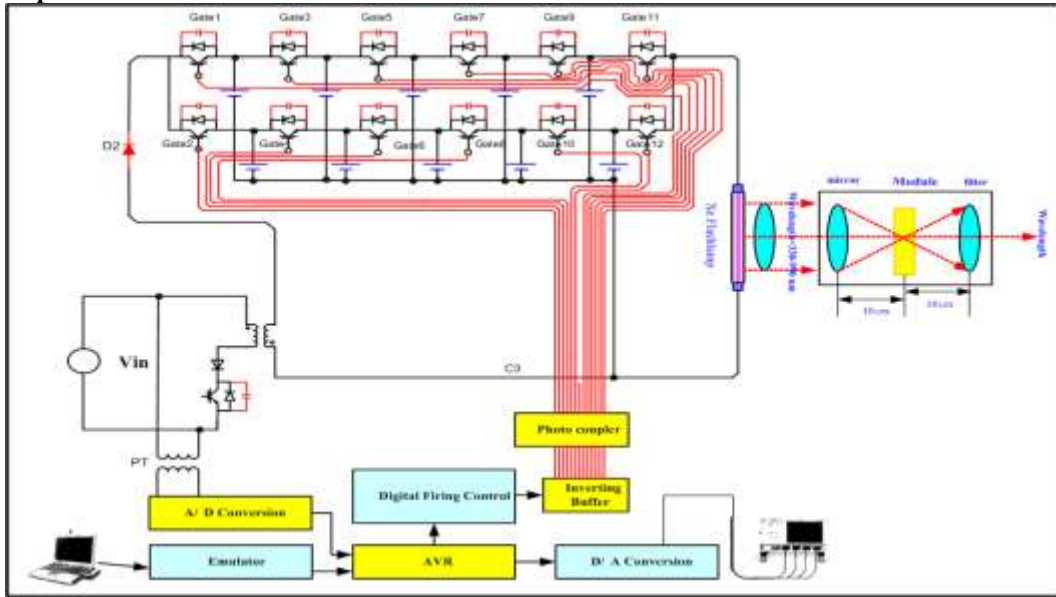


Fig. 1 IPL device that added a pulshesape, pulse superpositionby installing nonlinear optic crystal(KTP).

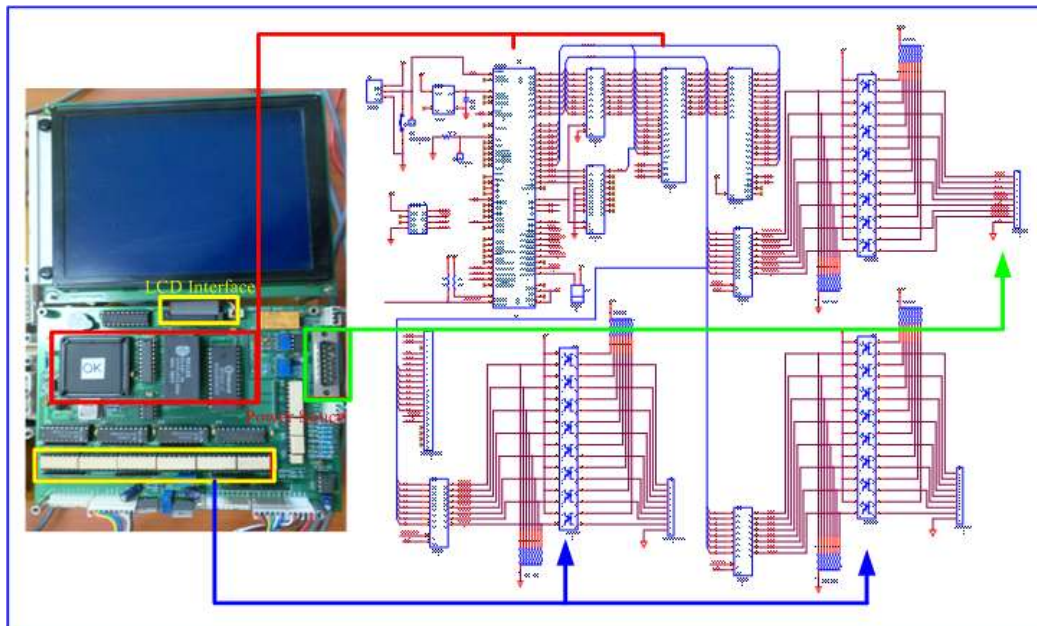


Fig. 2AT90S8535 one chip microprocessor on the ATMEL that is in charge of managing various types of control signals and the functions that operate the IPL device

As shown in figure 1, the power unit is composed of a simmer circuit, simmer starter, charging power supply and 6-layer mesh circuit to pre-light the Xe flash lamp, and of a 3-layer mesh circuit, which is composed of an overlapping circuit and pulse overlapping control circuit that can control the delay time. Figure 2 shows an AVR AT90S8535 one chip microprocessor on the ATMEL, which is in charge of managing a range of control signals and functions that operate the IPL device. In particular, the inductance L was manufactured with an air-core solenoid for variability to prevent magnetic saturation when a large pulse current was flowed.

For the trigger method, this study employed the simmer method, which has a range of benefits, such as extending the life of the flash lamp, controlling the lamp condition, increasing the efficiency, and lowering the voltage of permitted voltage. The following gives a summary of the operation of the circuit. When a trigger signal is applied to the IGBT gate, the recharged energy stored in the main circuit C is discharged in the lamp. After the pulse overlapping control circuit detects gate 2 being turned on, it sends out a turn on sign to gate 2 after a certain delay time. Fig 3, Schematic figure of intense pulse light with control boards. Figure 4(a) shows the primary electric current of the operating waveform and transformer that turns the IGBT gate on in the operating

pulse. Figure 4(b) shows the primary current waveform of a gate-on current waveform and transformer that turns on the operating pulse in the IGBT gate. Figure 2, 3, 4 Schematic figure of intense pulse light with control boards.

Therefore, the stair-type of pulse can be obtained when the overlapping waveform is permitted to the main waveform after a certain delay time by controlling the delay time of the overlapping waveform. Figure shows the detailed structure of the IPL and green light converter. A convex lens was installed so that the IPL beam lights on the nonlinear optic crystal accurately to increase the conversion efficiency. The focal distance of the convex lens is 100mm, i.e. the KTP crystal, SHG device, was placed on the precise position.

Through the design of the Multiple-Mesh Network, the pulse duration was controlled more accurately, and a multiple mesh circuit was used to make the upper part of the light pulse. The greatest benefit of the multiple mesh circuit is that it can produce an IPL pulse that is a long, normal mode with stable power. Most of the multiple mesh circuits use the complex type of circuit. In this format, the capacitance C of each mesh is identical, and the inductance L is similar. The following is the complex approximation equation formed by certain impedance, and the multiple mesh circuits are designed according to the order in the equation [10].

$$Z_n = (L_T / C_T)^{1/2} \quad (1)$$

$$t_p = 2 (L_T / C_T)^{1/2} \quad (2)$$

$$C_T = t_p / 2 Z_n \quad (3)$$

$$L_T = t_p Z_n / 2 \quad (4)$$

$$V = (2 E / C_T)^{1/2} \quad (5)$$

$$i_p = V_0 / 2 Z_n \quad (6)$$

Only if  $Z_n$  : impedance of electric network

$L_T$  : total inductance

$C_T$  : total capacitance

$t_p$  : pulse width

V : recharging voltage

E : lamp input energy

$i_p$  : maximum current

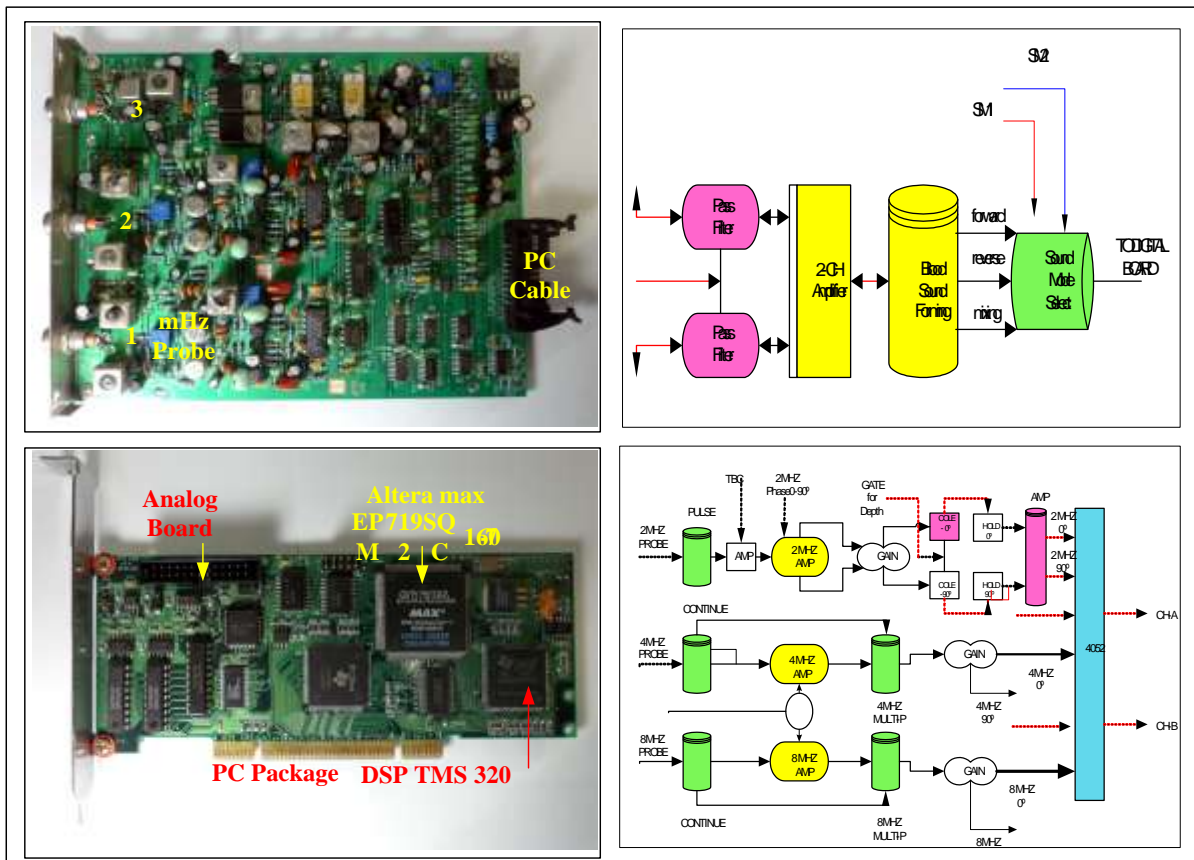
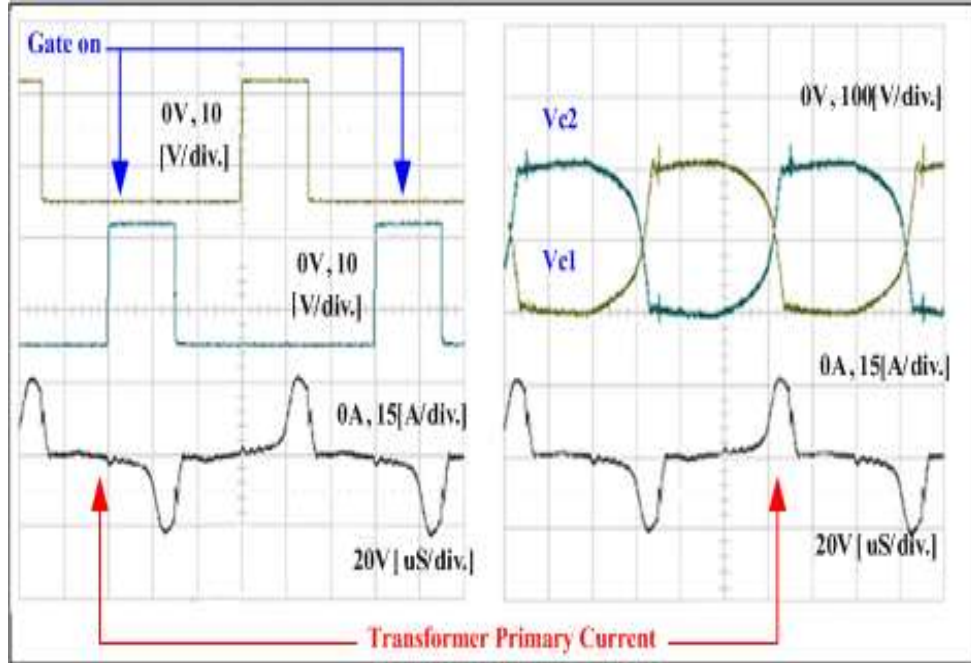


Fig. 3 Schematic figure of intense pulse light with control boards

### III EXPERIMENT RESULTS

As shown in Figure 1, the main circuit is composed of a 6-layer sing mesh circuit, and the square wave that is almost identical was obtained throughout the entire cycle. The main circuit was set with the capacitor  $C_1 \sim C_6$  of the mesh at  $60\mu\text{F}$ , the inductor  $L_1 \sim L_6$  at  $80\mu\text{H}$ , and the pulse width  $t_p$  of the current pulse waveform at  $\sim 1\text{ms}$ . The overlapping circuit was composed of a 3-layer mesh circuit, and a wave one similar to a sine wave was obtained.



**Fig. 4** (a) Primary electric current of the operating waveform and transformer that turns the IGBT gate on in the operating pulse., (b) Primary current waveform of gate-on current waveform and transformer that turns on the operating pulse in IGBT gate.

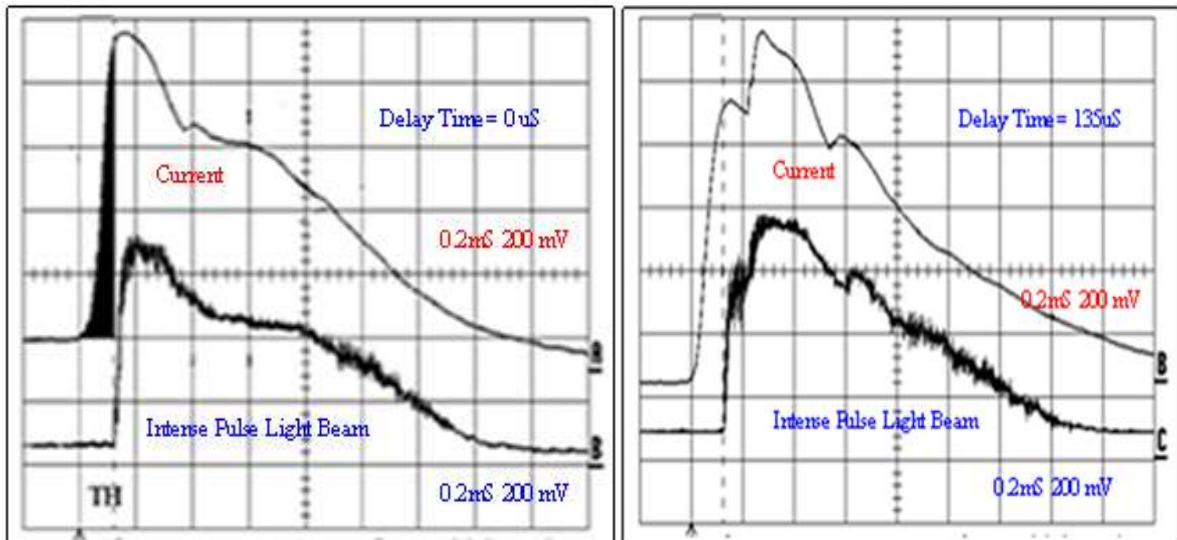


**Fig.5** Current waveform of the flash lamp and IPL-Beam when delay time =  $0\mu\text{s}$

**Fig. 6** Current waveform of the flash lamp and IPL-Beam when delay time =  $135\mu\text{s}$ .

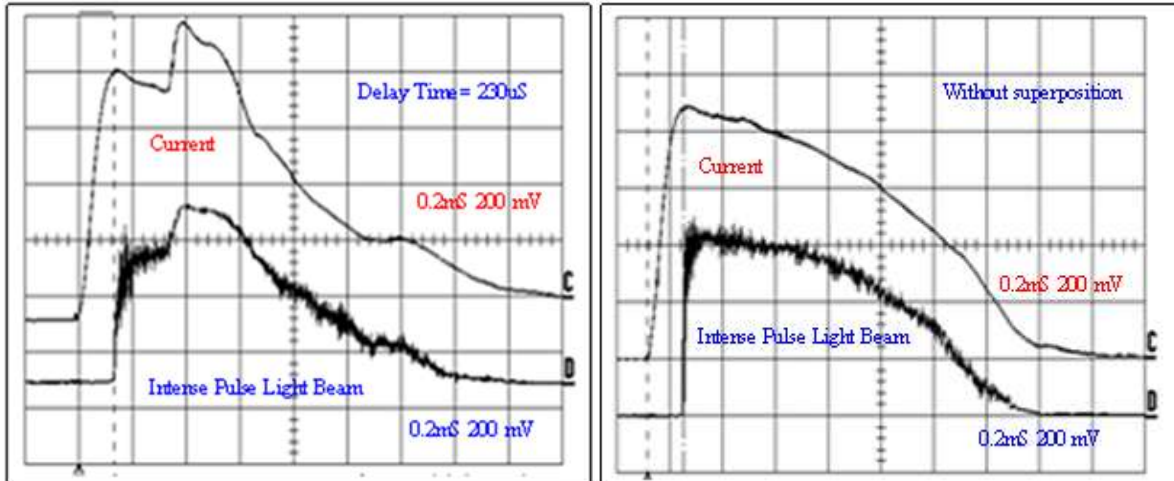


**Fig. 7** Current waveform of the flash lamp **Fig. 8** Current waveform of the flash lamp and IPL-Beam when delay time =230  $\mu$ s. and IPL-Beam when there is no superposition.

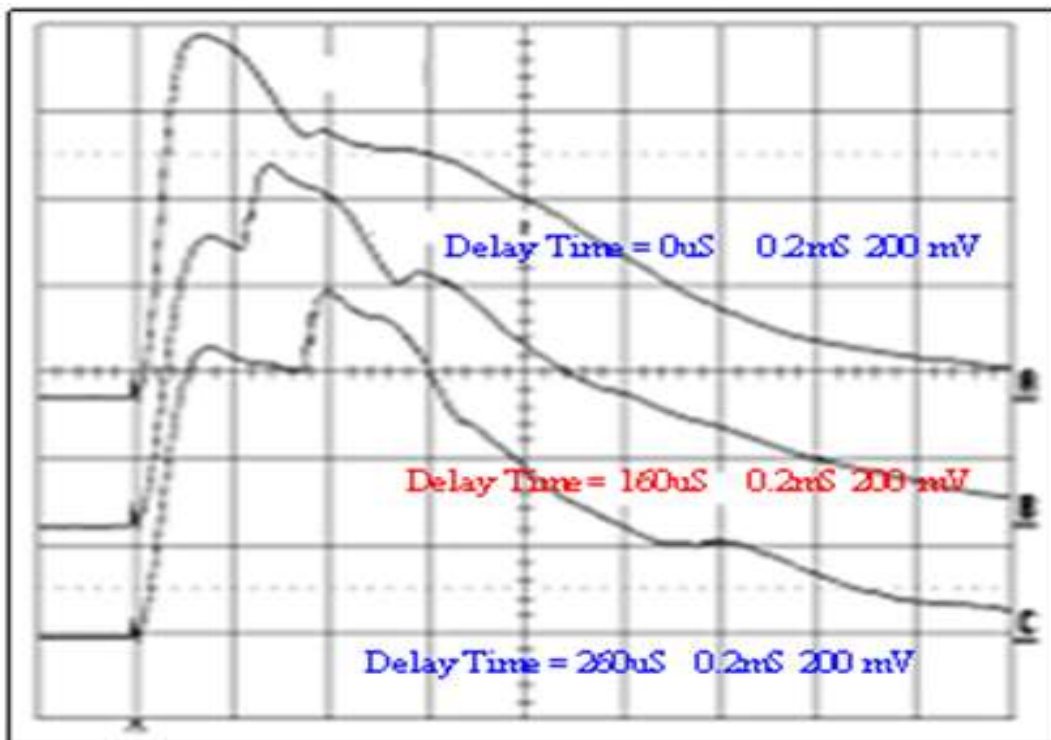


**Fig. 9** Current waveform of the flash lamp and IPL-Beam when delay time 0,160, 260  $\mu$ s

The overlapping circuit was set with the capacitor  $C_{10} \sim C_{30}$  of each mesh at  $40\mu$ F, the inductor  $L_{10} \sim L_{30}$  at  $30\mu$ , and the pulse width  $t_p$  of the current pulse waveform at  $\sim 0.2$ ms. Figure 5 Current waveform of the flash lamp and IPL-Beam when delay time =0  $\mu$ s. Figure 6 Current waveform of the flash lamp and IPL-Beam when delay time =135  $\mu$ s. Figure

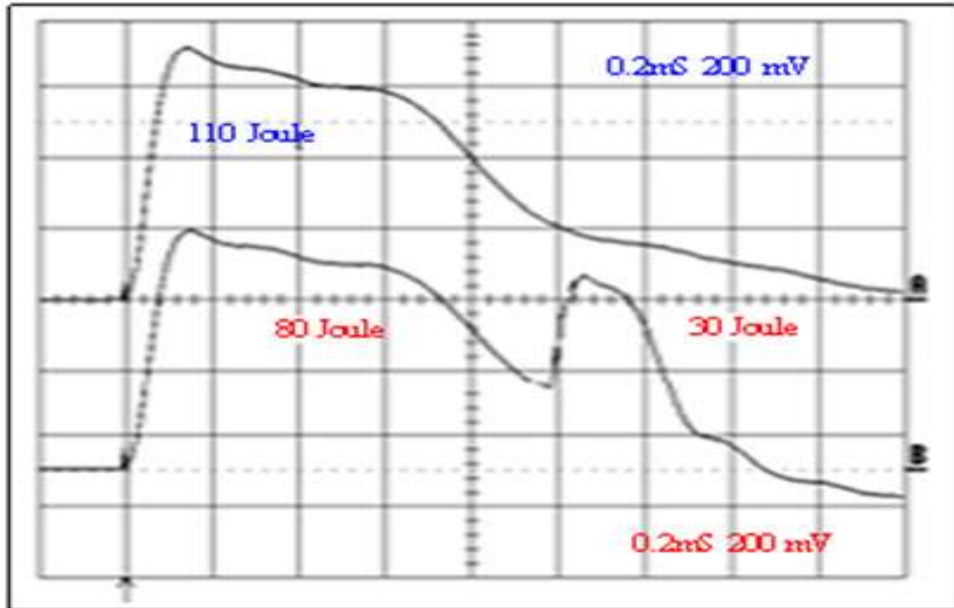


Fig. 10 Current waveform of the flash lamp and IPL-Beam 110 Joule when delay time 80, 30 joule

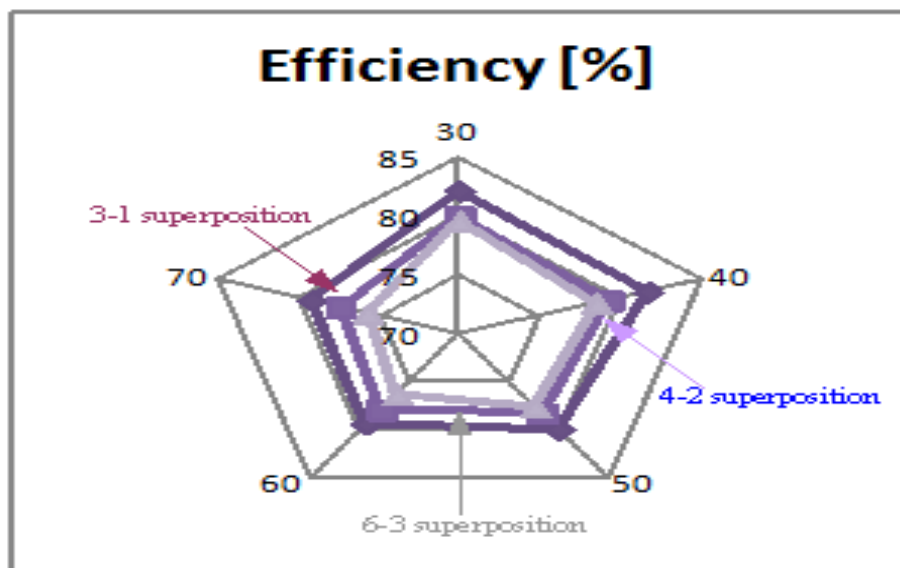


Fig. 11 Conversion efficiency of the measured IPL and superposition light output

7 Current waveform of the flash lamp and IPL-Beam when delay time =230  $\mu$ s. Figure 8 Current waveform of the flash lamp and IPL-Beam when there is no superposition. Figure 9 Current waveform of the flash lamp and IPL-Beam when delay time 0,160, 260  $\mu$ s. As shown in Figure 1, the main circuit consists of 1 ~ 6 layers of mesh, and the overlapping circuits have 1~6 layers of mesh. Figure 10 shows how the conversion efficiency was calculated.

The converted energy from 330 nm of IPL output and 165 nm of green light, each energy from the pulse overlapping circuits with 3~ 1 layers (main circuit-overlapping circuit), 4~2 layers and 6~3 layers was calculated. Figure 10 Current waveform of the flash lamp and IPL-Beam 110 Joule when delay time 80, 30 joule, the green light output after emission of the IPL output and nonlinear optic crystal was measured. As shown in Figure 11 Control board and intense pulse light hand peace body and power system. Output of light after penetrating the second harmonic generation and IPL output. The conversion efficiency of second harmonic generation light decreased with increasing input energy. The conversion property of green light in the 4~2 layered mesh was composed of 4 layers in the main circuit, and 2 layers of mesh in the overlapping circuit because the input energy was changed as each of them was permitted, the outputs of the IPL and green light were measured, and the conversion property is shown in Figure. Figure 11, Conversion efficiency of the

measured IPL and superposition light output. Conversion efficiency of the energy light based on the mesh number. The green light conversion characteristics of the 6-3 layered mesh was composed of 6 layers for the main circuit, and 3 layers of mesh for the overlapping circuit, and the conversion property of the IPL and green light outputs were measured as the input energy was changed as permitted.

The conversion efficiency into second harmonic generation decreased with increasing input energy. Figure shows the conversion efficiency of second harmonic generation light according to the number of meshes. The second harmonic generation light output and its conversion efficiency in the second harmonic generation device were the highest when 1-layer was overlapped onto 3-layers.

#### IV. CONCLUSION

An intense pulse light was constructed with applied multistep multi-circuit that was designed in the electric network method, and pulse shaping technology that can control the shape of the IPL beam pulse and current pulse form of the flash lamp was developed. The output characteristics of second harmonic generation light that penetrated through SHG device, which was installed at the output unit of IPL based on the stair-type of pulse form obtained through the delay time change of pulse overlapping rules, were examined.

When an identical input energy was permitted, the green light output of the 3 -1 layer (main circuit-overlapping circuit) was 10% higher than that of the 4-2 layered ones, and 30% higher than the 6-3 layered ones. As the input energy was increased from 33[J] to 73[J], in 10[J] steps, the conversion efficiency of second harmonic generation light decreased by 0.5%.

A comparison of the cases of permitting identical input energy without overlap, and the one with stair-type of pulse via overlap in terms of IPL output showed that the output energy of the IPL beam was larger when it was not overlapped due to a loss of high fluorescence when the delay time of the overlapping pulse was  $> 230\mu\text{s}$ . On the other hand, when the delay time of overlapping pulse was within  $230\mu\text{s}$ , the output energy of the IPL was higher when it was overlapped, and the output energy increased when the delay time ( $t_d$ ) was shorter.

#### ACKNOWLEDGEMENTS

This work was supported by **Pierce** College (U.S.A.) Grant 2017.

#### REFERENCES

- [1]. Inghilleri M, Berardelli A, Marchetti P, Manfredi M. Effects of diazepam, baclofen and thiopental on the silent period evoked by transcranial magnetic stimulation in humans. *Exp Brain Res*, 109(3):467.72. 1991.
- [2]. Sun-Seob Choi, "Chopper application for Magnetic Stimulation", *Journal of Magnetics*, Vol.15, No.4, 2010.
- [3]. Walsh V, Pascual-Leone A. *Transcranial magnetic stimulation: aneurochronometrics of mind*. Cambridge, MA: MIT Press; 2005.
- [4]. Wassermann E. *Oxford handbook of Transcranial magnetic stimulation*. Oxford: Oxford University Press; 2007.
- [5]. Frackowiak RSJ, Friston KJ, Frith C, et al. *Human brain function*. 2nd ed. San Diego: Academic Press; 2003.
- [6]. Sun-Seob Choi, "Transcranial Magnetic Stimulation with Applied Multistep Direct Current Grafting", *Biomedical Engineering: Applications, Basis and Communications*, Vol. 25, No. 4, 1350032,1-6. 2010.
- [7]. Nicole A.Lazar. *The Statiscal Analysis of FunctionalMRI Data*. Springer. 2008.
- [8]. Walter J. Levy. *Magnetic motor stimulation basic principles and clinical experience*. ELSEVIER
- [9]. Carl Senior. *Method in Mind*. The MIT Press.
- [10]. Sun-Seob Choi, "Treatment pulse application for Magnetic Stimulation", *journal of Biomedicine and Biotechnology*, article ID 278062, 6page, doi: 10.1153/2011/278062. 2011.
- [11]. Sun-Seob Choi, "Full Wave Cockroft Walton application for magnetic stimulation," *Journal of Magnetics*, Vol.16, No.3, September 2011, pp.246-252
- [12]. Wassermann E. *Oxford handbook of Transcranial magnetic stimulation*. Oxford: Oxford University Press; 2007.
- [13]. OrrinDevinsky, Aleksandar Beric. *Eectrical and magnetic stimulation of the brain and spinal cord*. Raven Press:
- [14]. Frackowiak RSJ, Friston KJ, Frith C, et al. *Human brain function*. 2nd ed. San Diego: Academic Press; 2003.
- [15]. Sun-Seob Choi, "Transcranial magnetic stimulation with applied multistep direct current grafting", *Biomedical Engineering: Applications, Basis and Communications*, Vol. 24, No.5, April 2013.
- [16]. Mark S.George. *Transcranial magnetic stimulation in clinical psychiatry*. American psychiatric publishing, inc.
- [17]. Walter J. Levy. *Magnetic motor stimulation basic principles and clinical experience*. ELSEVIER
- [18]. Walsh V, Pascual-Leone A. *Transcranial magnetic stimulation: a neurochronometrics of mind*. Cambridge, MA: MIT Press; 2005.
- [19]. Carl Senior. *Method in Mind*. The MIT Press.
- [20]. Pascal Wallisch. *MATLAB for Neuroscientists*. ACADEMIC PRESS.
- [21]. Sun-Seob Choi, "Treatment pulse application for Magnetic Stimulation", *journal of Biomedicine and Biotechnology*, Vol. 2011, article ID 278062, 6page, doi: 10.1153/2011/278062.